Hydrogen Bonding Modulates Binding of Exogenous Ligands in a Myoglobin Proximal Cavity Mutant†

Sean M. Decatur,‡ Kristin L. Belcher,‡ Paula K. Rickert,§ Stefan Franzen,§,|| and Steven G. Boxer*,§

Departments of Chemistry, Stanford University, Stanford, California 94305-5080, and Mount Holyoke College, South Hadley, Massachusetts 01075-6407

Received April 19, 1999; Revised Manuscript Received June 11, 1999

ABSTRACT: In the sperm whale myoglobin mutant H93G, the proximal histidine is replaced by glycine, leaving a cavity in which exogenous imidazole can bind and ligate the heme iron (Barrick, D. (1994) *Biochemistry 33*, 6545−6554). Structural studies of this mutant suggest that serine 92 may play an important role in imidazole binding by serving as a hydrogen bond acceptor. Serine 92 is highly conserved in myoglobins, forming a well-characterized weak hydrogen bond with the proximal histidine in the native protein. We have probed the importance of this hydrogen bond through studies of the double mutants S92A/H93G and S92T/H93G incorporating exogenous imidazole and methylimidazoles. ^{1}H NMR spectra reveal that loss of the hydrogen bond in S92A/H93G does not affect the conformation of the bound imidazole. However, the binding constants for imidazoles to the ferrous nitrosyl complex of S92A/H93G are much weaker than in H93G. These results are discussed in terms of hydrogen bonding and steric packing within the proximal cavity. The results also highlight the importance of the trans diatomic ligand in altering the binding and sensitivity to perturbation of the ligand in the proximal cavity.

Exogenous molecules which serve a specific structural or functional role can be inserted into engineered protein cavities as an extension of site-directed mutagenesis for dissecting protein structure−function relationships in heme proteins (*1*−*4*). When a residue which ligates the heme iron (such as histidine) is mutated to a smaller, nonligating amino acid (typically alanine or glycine), exogenous molecules which may mimic natural amino acids side chains or bear nonnatural functionality can be introduced into the resulting cavity and incorporated into the protein structure. For example, in sperm whale myoglobin (Mb[1]), the proximal histidine (His 93) is the sole covalent linkage between the polypeptide chain and the heme iron. In the mutant H93G, this residue has been replaced by glycine, creating a cavity in the proximal heme pocket. When H93G Mb is expressed in *Escherichia coli* in the presence of imidazole, the protein is isolated with an imidazole molecule occupying that cavity and serving as an axial ligand to the heme iron (*1*). This imidazole can be replaced with a variety of exogenous ligands via a simple dialysis technique, producing protein complexes that are distinguishable by many physical observables (*2*, *5*−*7*). These proteins are denoted H93G(L), where L represents the bound proximal ligand, and they are hybrids of model compounds and site-directed mutants. As in model compounds, the heme ligand can be systematically varied beyond the limited range of the naturally occurring amino acids, but because the protein architecture is preserved, interactions between the polypeptide and the heme ligand can also be studied.

The most striking difference between the structures of metaquoH93G(Im) and wild-type myoglobin (WTMb) is in the conformation of the proximal imidazole ring. The exogenous proximal imidazole of H93G(Im) is rotated about the Fe−N_i bond by about 40° relative to the imidazole of His 93 of WTMb; instead of eclipsing the pyrrole nitrogens of the heme as in WTMb, the imidazole ring is nearly aligned with the heme *meso* carbons (*1*; Figure 1). This rotation is confirmed in solution by the pattern of heme methyl hyperfine shifts in the ^{1}H NMR spectrum of H93G(Im)CN and by the positions of the heme methine protons in the diamagnetic CO complex (*5*). The cause of this rotation is unknown, but it suggests that the orientation of the histidine side chain in the wild type is constrained by the covalent link to the polypeptide backbone, perhaps preventing the proximal heme pocket from adopting its most stable conformation. For example, when the imidazole ring eclipses the *meso* carbons instead of the pyrrole nitrogens, there is less steric repulsion between the imidazole and the heme; thus, this rotation of the imidazole ring in H93G(Im) is likely correlated with a shorter Fe−N_i bond length (*1*).

The rotation of the Im ring may also optimize its interactions with amino acids of the proximal heme pocket. In the H93G(Im) complex, the distance between the Im N_ϵ and the O_γ of Ser 92 is 2.7 Å (*1*) suggesting that a hydrogen bond between the Im and Ser 92 might be important in

† This work is supported in part by Grant GM27738 from the National Institutes of Health (to S.G.B.) and a Camille and Henry Dreyfus Foundation New Faculty Award and Research Corp. Cottrell College Award (to S.M.D.).

* To whom correspondence should be addressed.

‡ Mount Holyoke College.

§ Stanford University.

|| Current address: Department of Chemistry, North Carolina State University, Raleigh, NC 27695-8204.

[1] Abbreviations: Mb, myoglobin; L, proximal ligand; H93G(L), H93G myoglobin with "L" as proximal ligand; Im, imidazole; MeIm, methylimidazole; WT, wild type; MbCN, metcyanomyoglobin; MbNO, nitrosylmyoglobin.

10.1021/bi9908888 CCC: $18.00
Published on Web 07/31/1999

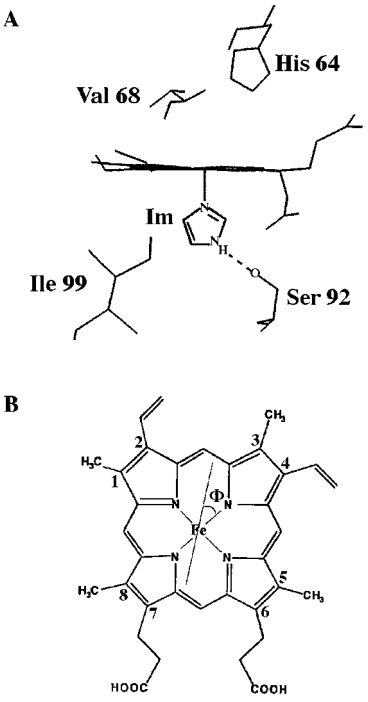

FIGURE 1: (A) Schematic diagram of the proximal cavity in H93G(Im) depicting the hydrogen bond between Ser 92 and the proximal Im, based on the X-ray crystal structure of metaquoH93G(Im) (*1*). (B) Schematic of the heme, with the numbering system used in the NMR assignments.

stabilizing the binding and conformation of the Im ligand (Figure 1). Strong hydrogen bonding between the proximal ligand and surrounding amino acids can have a significant effect on the electronic structure and function of the heme. For example, a strong hydrogen bond between the proximal histidine (His 174) and the carboxylate of a nearby aspartate residue (Asp 235) in cytochrome *c* peroxidase is the primary cause of this enzyme's unusually low redox potential (*8*). The structural and functional consequences of a hydrogen bond between residue 92 and proximal His 93 have been studied extensively in Mb. In a neutron diffraction study of MbCO, Cheng and Schoenburn reported that the distance between the His 93 N_ϵ and Ser 92 O_γ is 3.2 Å, and the distance between the $N_\epsilon H$ and O_γ is 2.5 Å; on the basis of these data, they proposed that a weak hydrogen bond exists between His 93 $N_\epsilon H$ and Ser 92 O_γ (*9*). To test the importance of this hydrogen bond to the both the conformation of His 93 and protein function, Ser 92 has been changed to alanine and valine in porcine Mb (*10*), alanine and aspartate in human and horse heart Mbs (*11*, *12*), and alanine and proline in sperm whale Mb (*13, 14*). In all of the S92A Mbs, only modest changes in the orientation of the proximal His and the binding of diatomic ligands on the distal side were observed.

The H93G system presents the opportunity to further probe the importance of interactions between Ser 92 and the proximal imidazole. Because the Im N_ϵ and Ser 92 O_γ are closer in H93G than in WTMb, this residue may have a more significant impact on the imidazole conformation and/or the electronic structure of the heme. We have tested the significance of this interaction in H93G using two different strategies. First Im, which is a hydrogen bond donor when ligated to the heme iron, can be replaced with *N*-methylimidazole (*N*-MeIm), which cannot donate a hydrogen bond. In previous reports, we have shown that *N*-MeIm binds to H93G−CN and H93G−NO more weakly than Im and 4-MeIm (*5, 7*). Because *N*-MeIm and 4-methylimidazole (4-MeIm) are isosteric and have similar pK_a values, these differences in binding constants may be due to the differences in hydrogen bonding properties of these two ligands. Furthermore, both ν_{CO} and the CO on- and off-rates in H93G(4MeIm)CO suggest a more electron-rich iron than in H93G(NMeIm)CO, the expected effect of the loss of a hydrogen bond at the proximal ligand (*6*).

In this paper, we have adopted a second strategy: the hydrogen bond between the proximal ligand is altered by replacement of Ser 92 with alanine and threonine. By introducing the S92A mutation into the H93G protein, we remove the hydrogen bond with the Im; by replacing the serine with a threonine (S92T), we change the position of the hydroxyl group and, therefore, can modulate either the strength of the hydrogen bond or the conformation of the imidazole ring.

^{1}H NMR spectroscopy of the metcyano complexes provides a great deal of information about the structure and dynamics of these mutants. MbCN is a paramagnetic ($S = {}^1/_2$) species; the hyperfine shifts of protons of the heme and amino acids of the heme pocket are very sensitive to changes in conformation of the proximal ligand (*15*−*17*). Each new exogenous ligand in H93G gives a unique fingerprint hyperfine shifted region of the MbCN ^{1}H NMR spectrum (*2*). The assignments for some protons of the heme and heme pocket amino acids in H93G(Im)CN, H93G(*N*-MeIm)CN, H93G(4-MeIm)CN, and H93G(2-MeIm)CN have been presented (*5*). In this paper, we report the assignments for these protons, as well as ligand and proton exchange dynamics, in the S92A/H93G(Im)CN and S92T/H93G(Im)CN complexes. In a previous study (*4*) binding constants for exogenous imidazoles to the nitrosyl complex of H93G were reported; in this paper we have extended those studies to the S92A/H93G and S92T/H93G proteins. Taken together, these data describe the role of Ser 92 in determining the conformation of the bound Im, the dynamics and accessibility of the proximal cavity, and the binding affinities of different imidazoles. Furthermore, these data demonstrate the utility of the functional cavity approach for dissecting the importance of polypeptide−heme ligand interactions.

MATERIALS AND METHODS

Plasmids encoding for the double mutants S92T/H93G and S92A/H93G were prepared using cassette mutagenesis. The double mutants and H93G(Im) were purified from *E. coli* as described elsewhere (*1, 2*).

^{1}H NMR Experiments. ^{1}H NMR samples were prepared as described earlier (*5*). Protein concentrations were typically between 1 and 3 mM in 100% D_2O, 0.1 M phosphate, pH = 7.0 buffer, or 90% H_2O/10%D_2O, 0.1 M phosphate, pH = 9.4 buffer (the pH meter readings are uncorrected for the isotope effect). All ^{1}H NMR spectra were recorded on a GE Omega 500 MHz spectrometer. Spectra were routinely measured at 30 °C with saturation of the residual water signal with the decoupler channel during the predelay period. Absolute value COSY (MCOSY) and phase-sensitive NOESY spectra were acquired as described earlier (*3*). Proton exchange rates were measured using the saturation transfer

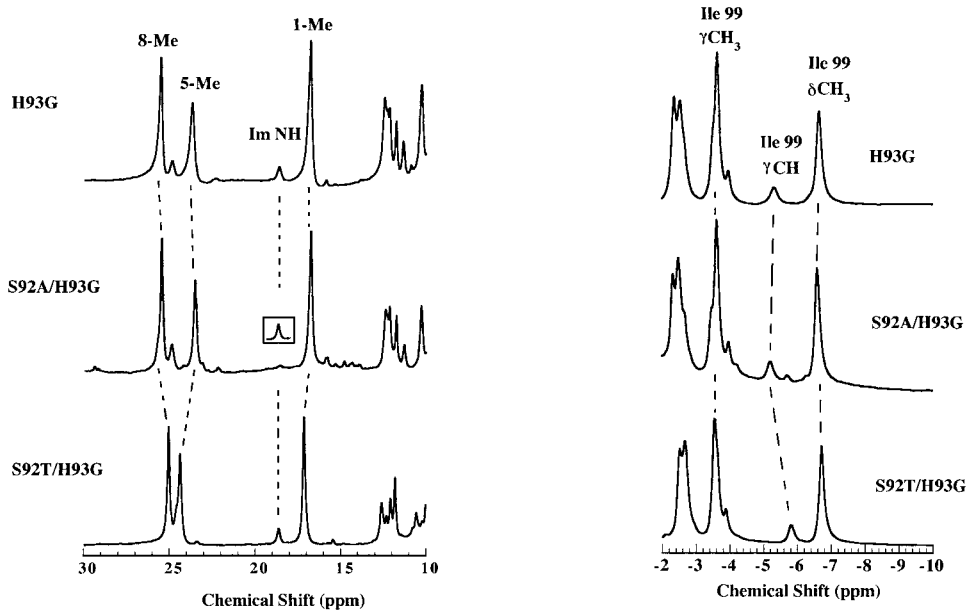

FIGURE 2: Downfield (A) and upfield (B) hyperfine-shifted regions of the 500 MHz ^{1}H NMR spectra of H93G(Im)CN, S92A/H93G(Im)-CN, and S92T/H93G(Im)CN with water presaturation. The inset in the spectrum for S92A/H93G(Im)CN is the Im NH proton seen in the absence of water presaturation. Assignments are listed in Table 1.

method, as described by Lecomte and La Mar (*18*). Protein samples were prepared in 90% H_2O/10% D_2O buffer. Spectra were collected at several pH values over the range 9.4−7.0. The pH was adjusted by adding 0.1 M HCl to the sample and measuring the pH using a meter equipped with an Ingold microelectrode. To suppress the intensity of the water signal, the 1−1 pulse sequence was used (*19*). The decoupler was applied to the water peak causing saturation or to an off-resonance frequency during nonacquisition times. The intensity of the Im NH proton was measured in the on-resonance (I) and off-resonance (I_o) spectra, giving a saturation factor $F = I/I_o$. The rates of exchange (τ^{-1}) were determined from the saturation factors using the expression

$$\tau^{-1} = \rho(1 - F)/F \qquad (1)$$

where ρ is the intrinsic relaxation rate of the proton. The intrinsic lifetime was determined by measuring T_1 at pH 7, where the exchange rate τ^{-1} is much slower than the T_1 relaxation rate (*18*). T_1 was measured using a 180°−t−90° inversion−recovery sequence, with saturation of the water peak at all times except during acquisition. T_1 was calculated from the slope of plots of $\log[I_\infty - I(t))/2I_\infty]$ versus t (*15, 20*).

Ligand exchange rates were determined by measuring the spectral changes which occur after addition of an excess of deuterated exogenous ligand to the sample. As the protonated ligand bound to the protein exchanges for the deuterated ligand, the disappearance of resonances from protons of protein-bound ligand can be analyzed to give the ligand exchange rate (*5*). Deuterated Im was purchased from Cambridge Isotope Laboratories; deuterated *N*-methylimidazole (4,5-d_2) was a gift of John Williams and Dr. Anne McDermott.

Binding of Imidazoles to NO Complexes. A 1 cm quartz cuvette was filled with 2 mL of buffer (0.1 M phosphate pH 7), sealed with a rubber septum, and purged with N_2 for about 10 min. A small amount (~10 μL) of protein from a stock solution was added to the cuvette, along with a minimal amount of sodium dithionite from a freshly prepared 1 M solution. The cuvette was then briefly placed under a stream of NO gas to produce the NO complex. The UV/vis spectrum of the sample was measured on a Pharmacia Ultrospec 4000 spectrophotometer. Titration of the protein−NO complex with various imidazoles was monitored by changes in the UV/vis spectra as described previously (*6*).

RESULTS

Assignments of S92T/H93G(Im)CN and S92A/H93G(Im)-CN. The ^{1}H NMR spectra of H93G(Im)CN, S92A/H93G-(Im)CN (in 95% H_2O, pH 9.4), and S92T/H93G(Im)CN are aligned in Figure 2 (see Table 1). Overall, the spectra of H93G(Im)CN and S92A/H93G (Im)CN are nearly identical, and the assignments for H93G(Im)CN can be extended to S92A/H93G(Im)CN. The S92T/H93G(Im)CN spectrum is slightly different from that of H93G(Im)CN, with shifts observed in the heme 8-Me and 5-Me resonances. The assignments for S92T/H93G(Im)CN were confirmed by following the method used for H93G(Im)CN (*5*).

Imidazole NH Proton Exchange Rates. The spectra in Figure 2 were obtained with presaturation of the water resonance. While the Im NH proton is well resolved in the H93G(Im)CN and S92T/H93G(Im)CN spectra, in S92A/H93G(Im)CN this peak is lost in the baseline and is only visible in the absence of water presaturation (see Figure 2 inset) or at a pH close to 7. This pH-dependent saturation transfer from the water to the proximal Im NH occurs because of base-catalyzed proton exchange (*18, 21*).

While the resonance in S92A/H93G(Im)CN is completely saturated at pH 9.4, only partial saturation occurs for H93G-(Im)CN and S92T/H93G(Im)CN, and in these proteins the exchange rates can be measured by saturation transfer. The saturation factors F, where $F = I/I_0$, for H93G and S92T/H93G are plotted versus pH in Figure 3A. All three mutants have $F = 1.0$ at pH 7.0, indicating that the rate of exchange is much slower than the intrinsic spin relaxation rate at this

Table 1: Proton Chemical Shift Assignments for Im Complexes of H93G, S92A/H93G, and H93G/S92T in the Met Cyano Form

proton		H93G(Im)CN [a]	S92A/ H93G(Im)CN	S92T/ H93G(Im)CN
heme	8-Me	25.6	25.6	25.3
5-Me	5-Me	23.6	23.6	24.7
	1-Me	16.7	16.7	17.0
	2-α	11.4	11.4	11.9
	2-β	−0.34	−0.34	−0.45
		0.48	0.48	0.41
	4-α	10.2	10.2	9.88
	4-β	−3.88	−3.88	−3.78
		−2.54	−2.54	−2.45
Im	C4H	12.1	12.1	12.0
	N1H	18.7	18.7	
Ile 99	CβH	0.28	0.28	0.10
	CγH	−5.33	−5.33	−5.91
		−3.67	−3.67	−3.61
	CγH$_3$	−3.48	−3.48	−2.71
	CδH$_3$	−6.68	−6.68	−6.75
Gly 93	CαHs	6.77	6.77	
	N$_b$H	12.2	12.2	12.2
Phe 43	CδHs	8.57	8.57	8.7
	CϵHs	12.4	12.4	12.6
	CζH	16.9	16.9	17.1
His 64	NϵH	24.8	24.8	24.8

[a] Taken from ref *5*.

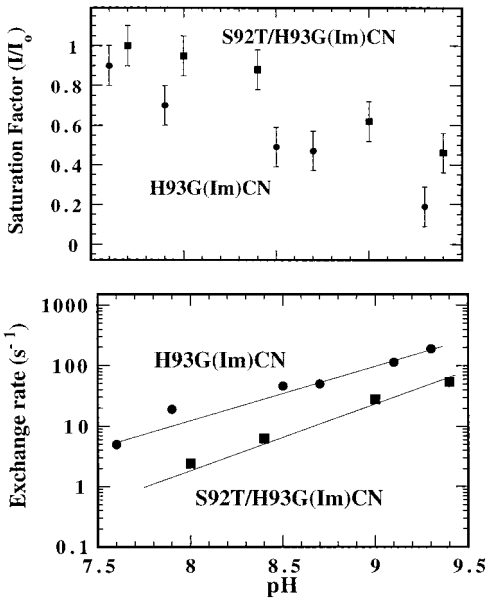

FIGURE 3: (A) Saturation factors (I/I_o) for the Im N−H proton in the Mb cavity mutants. (B) Proton exchange rates for Im N−H proton in Mb cavity mutants, calculated using eq 1, where $\rho^{-1} =$ 22 ms. The lines are shown to guide the eye.

pH. Saturation factors for S92T/H93G are larger than those of H93G and S92A/H93G throughout the entire pH range. The intrinsic spin relaxation time ρ^{-1} for the Im NH proton was measured as 22 ms in all three mutants. Using the values for ρ and F in eq 1, the exchange rates τ^{-1} were calculated and are plotted in Figure 3B. The exchange rates for S92T/H93G and H93G lie on nearly parallel lines, with S92T/H93G having a slower proton exchange rate across the entire pH range.

Exogenous Imidazole Exchange Rates in S92A/H93G and S92T/H93G. When an excess of deuterated Im (Im-d_3) is added to an S92A/H93G(Im)CN sample, the resonance for the Im C$_4$H proton at 12.1 ppm disappears over time (Figure

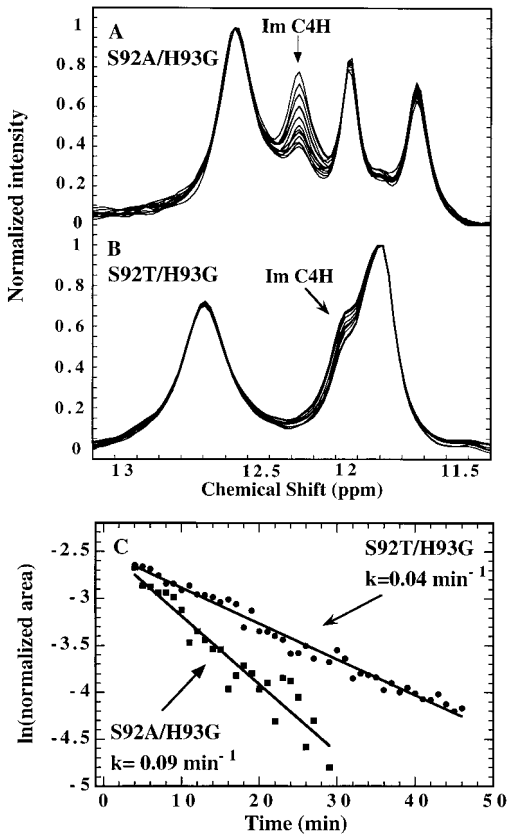

FIGURE 4: 500 MHz ^{1}H NMR spectra of (A) S92A/H93G(Im)CN and (B) S92T/H93G(Im)CN taken after addition of Im-d_3 to the NMR sample. Spectra were measured at 1 min intervals and are shown normalized to the Phe43 CϵH peak. (C) Decays of the integrated area of the Im C$_4$H peak over time. The decays are single exponential and are fit to give $k_{ex} = 0.09$ min^{-1} for S92A/H93G and 0.04 min^{-1} for S92T/H93G.

Table 2: Exogenous Ligand Exchange Rates in Met Cyano Complexes of Mb Cavity Mutants

cavity mutant	ligand	k_{ex} (min^{-1})
H93G	imidazole	0.09 ± 0.01
S92A/H93G	imidazole	0.09 ± 0.01
S92T/H93G	imidazole	0.04 ± 0.01
H93G	*N*-methylimidazole	0.17 ± 0.01

4A). The rate of exchange of Im for Im-d_3 is 0.09 min^{-1} (Figure 4C), the same as in H93G (*5*). In S92T/H93G, the Im C$_4$H proton is less well resolved, appearing as a shoulder to the resonance of the heme 2-a proton; however, the disappearance of this shoulder upon addition of Im-d_3 is still clearly discernible (Figure 4B). The ligand exchange rate for S92T/H93G(Im)CN is $k = 0.04$ min^{-1} (Figure 4C), significantly slower than that of H93G and S92A/H93G (Table 2).

Binding of Methylimidazoles to Metcyano Complexes. The spectra of the *N*-MeIm complexes of H93G, H93G/S92A, and H93G/S92T are aligned in Figure 5. The spectra for all three mutants are nearly identical, and the assignments for H93G(*N*-MeIm)CN can be extended to the double mutants as well (Table 3). The similarity in the spectra suggests that the conformation of the *N*-MeIm is the same in all three mutants. By addition of deuterated *N*-MeIm (4,5-d_2 *N*-MeIm) to a sample of H93G(*N*-MeIm)CN, the rate of exchange of *N*-MeIm can be measured. The NMR spectra of H93G(*N*-MeIm)CN upon addition of 4,5-d_2 *N*-MeIm are shown in

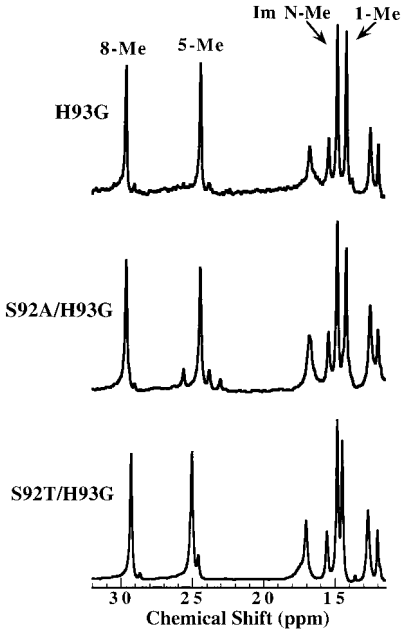

FIGURE 5: Downfield hyperfine shifted region of the 500 MHz ^{1}H NMR spectra of H93G(*N*-MeIm)CN, S92A/H93G(*N*-MeIm)CN, and S92T/H93G(*N*-MeIm)CN. Assignments are listed in Table 3.

Table 3: Proton Chemical Shift Assignments of Selected Downfield Hyperfine Shifted Resonances in *N*-MeIm Complexes of H93G, H93G/S92A, and H93G/S92T

proton		H93G [a]	S92T/H93G	S92T/H93G
heme	8-Me	29.6	29.6	29.3
	5-Me	24.4	24.4	24.2
	1-Me	14.2	14.2	14.5
N-MeIm	Me	14.8	14.8	14.8
	C4H	15.5	15.5	15.6
His 64	NH	25.4	25.4	25.4
Phe 43	CζH	16.7	16.7	17.0
	CϵHs	12.4	12.4	12.6

[a] H93G data taken from ref *5*.

Figure 6A; the peak at 15.5 ppm disappears over time as protonated *N*-MeIm exchanges for the deuterated ligand. The rate for this process is determined to be 0.170 min^{-1}, almost a factor of 2 faster than the rate of Im exchange.

Binding of Imidazole and Methylimidazoles to Nitrosyl Complexes. Addition of NO to deoxyH93G(L) at low [L] gives the five-coordinate NO complex denoted H93G−NO as indicated by the broad Soret band at 400 nm and EPR data (*6*). Upon addition of excess imidazole or methylimidazole, the Soret band shifts from 400 to 420 nm as the six-coordinate H93G(L)NO complex is formed:

$$\text{H93G}-\text{NO} + \text{L} \rightleftharpoons \text{H93G(L)NO} \quad (2)$$

$$K = \frac{[\text{H93G(L)NO}]}{[\text{H93G}-\text{NO}][\text{L}]} \quad (3)$$

A plot of the change in absorbance at 420 nm ($\Delta A_{420} = A([\text{Im}]) - A([\text{Im}] = 0)$) versus $\Delta A_{420}/[\text{Im}]$ results in a straight line with slope $1/K$:

$$\Delta A = \text{constant} + \frac{\Delta A}{[\text{L}]}K^{-1} \quad (4)$$

Data for binding of Im, 4-MeIm, and *N*-MeIm to the NO complexes are given in Figure 7 and Table 4. The binding

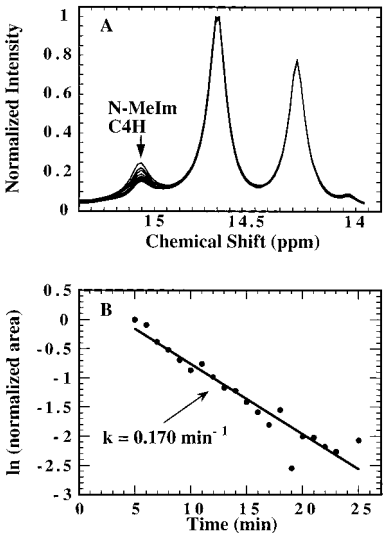

FIGURE 6: (A) 500 MHz ^{1}H NMR spectra of H93G(*N*-MeIm)CN taken after addition of 4,5-d_2 *N*-MeIm to the NMR sample. Spectra were measured at 1 min intervals and are shown normalized to the Phe43 CϵH peak at 12.4 ppm. (B) Decay of integrated area of the *N*-MeIm C_4H peak over time. The decay is a single exponential and can be fit to give $k_{ex} = 0.17$ min^{-1}.

constants of exogenous ligands to H93G−NO and S92T/H93G−NO are very similar, but binding to S92A/H93G−NO is weaker by over 1 order of magnitude. Furthermore, while H93G−NO and S92T/H93G−NO bind 4-MeIm more tightly than *N*-MeIm, S92A/H93G−NO binds the two methylimidazoles with comparable affinity.

DISCUSSION

The ^{1}H NMR data on the metcyano complexes of both serine 92/H93G double mutants, combined with UV/vis titrations on the nitrosyl complexes, provide a basis for understanding the effect of residue 92 on the conformation, dynamics, and binding affinities of exogenous imidazoles to the proximal cavity of H93G. Mutation of serine 92 to alanine or threonine can have two possible effects on the conformation and properties of the proximal cavity. First, the three residues differ in their possible hydrogen bonding interactions with the proximal imidazole. The S92A mutation removes a possible hydrogen bond acceptor. This may weaken interactions between exogenous ligands and the proximal cavity and affect bonding between ligands and the heme iron as the hydrogen-bonded imidazole has a higher effective pK_a, making it a better ligand for the heme iron (*22*−*24*). Second, the three residues differ in size (Thr > Ser> Ala) and thus differ in the packing or steric interactions within the proximal cavity. S92A/H93G is expected to have the most spacious cavity, perhaps associated with the greatest accessibility to penetration by solvent or proximal ligands, while S92T/H93G should have the most crowded cavity.

Ser 92 Has Little Effect on Im Conformation. The hyperfine shifts in the ^{1}H NMR spectra of MbCN complexes are very sensitive to changes in heme axial ligand conformation, and comparisons of these shifts in different mutants can be used to assess changes in conformation of heme ligands and the local amino acid environment (*5, 13, 15*−*17*). For example, this pattern is very different in WT MbCN and H93G(Im)CN (*5*). Since S92A/H93G(Im)CN has a spectrum identical to that of H93G(Im)CN, the conformation

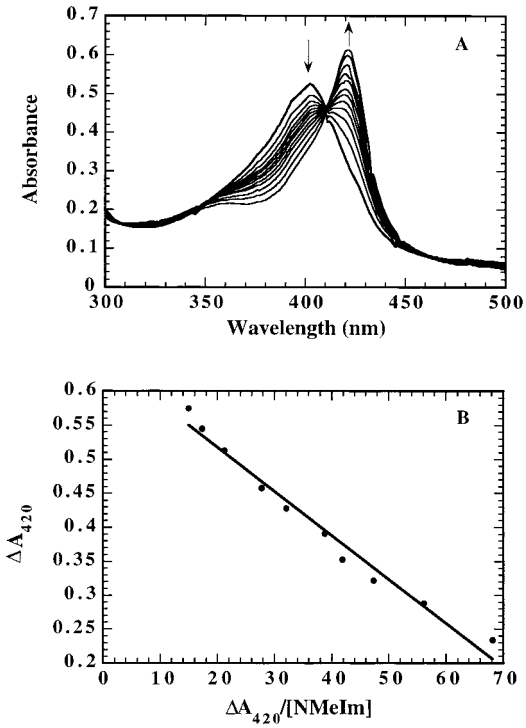

FIGURE 7: (A) UV/vis spectra of S92T/H93G−NO upon titration of *N*-MeIm. Binding of *N*-MeIm causes the Soret band to shift from 400 to 420 nm. (B) Plot of ΔA_{420} vs ΔA_{420}/[*N*-MeIm]. *K* is determined using eq 4. Imidazole concentrations were corrected for the fraction of protonated imidazole (ImH^+) present at pH 7.

Table 4: Binding Constants of Im, *N*-MeIm, and 4-MeIm to Nitrosyl Complexes of Mb Cavity Mutants with *K* Defined by Eqs 2 and 3

cavity mutant	K_{Im}	K_{N-MeIm}	K_{4-MeIm}
H93G[a]	1500	700	2000
S92A/H93G	10 ± 5	70 ± 20	60 ± 20
S92T/H93	1600 ± 200	1000 ± 200	2900 ± 500

[a] H93G data taken from ref *7*.

of the Im must be very similar in both complexes. Thus, *neither the loss of the hydrogen bond or the change to the size/packing of the cavity in S92A/H93G significantly impacts the conformation of the bound imidazole*.

There are some subtle differences in the spectrum of S92T/H93G(Im)CN compared to H93G(Im)CN. Threonine is a larger residue than serine, and there must be small changes on the proximal side that accommodate the extra methyl group. The small magnitude of the changes in the NMR spectrum suggests that the overall conformation of the ligand is still very similar to that found in H93G(Im).

Im NH Proton Exchanges More Rapidly in S92A/H93G. The rate-limiting steps in proton exchange for buried imidazoles can be penetration of solvent into the protein interior or local unfolding (such as disruption of hydrogen bonds) which is necessary to expose the group for exchange. Proton exchange rates therefore contain a great deal of information about the accessibility of an imidazole side chain and the local dynamic motions within the protein. Proton exchange for an imidazole ligated to the heme can occur by a base-catalyzed mechanism (*18*).[2] Thus, the differences in proton exchange behavior between H93G and the two double mutants reflect differences in accessibility of the proton.

The Im NH proton exchange rate is fastest for S92A/H93G and slowest for S92T/H93G (Figures 2 and 3). Thus, the Im NH proton is most accessible to solvent in S92A/H93G and most protected in S92T/H93G. The changes in accessibility of the Im NH proton can be explained in terms of changes in hydrogen bonding or in packing within the proximal cavity. The absence of a hydrogen bond in S92A/H93G-(Im) would leave the proton more accessible for exchange than in H93G(Im). Alternatively, the mutations to residue 92 can change the packing within the proximal cavity, increasing or decreasing barriers for solvent entry. Replacement of serine with a smaller residue (alanine) may make the cavity more accessible to solvent (faster proton exchange), while replacement with a larger residue (threonine) may increase the barrier for solvent penetration (slower proton exchange).

N-MeIm Has a Faster Ligand Exchange Rate Than Im. In earlier papers (*5*, *7*), we reported that the rate of exchange of Im with Im-d_3 is independent of the concentration of Im-d_3 and is very sensitive to the iron oxidation state and nature of the *distal* ligand (CN^- vs CO). One mechanism that would explain these observations is if the rate-determining step in ligand exchange is the off rate. In this paper, we also report the kinetics of replacement of *N*-MeIm by 4,5-d_2 *N*-MeIm in H93G(*N*-MeIm)CN. *N*-MeIm exchange is faster than Im. Since Im binds more strongly than *N*-MeIm, *N*-MeIm would be expected to have a faster off rate than Im. Thus, this observation is consistent with the interpretation of k_{ex} as the ligand off rate.

Effect of Ser 92 on Im Exchange Rates. Comparison of the Im exchange rates in H93G, S92A/H93G, and S92T/H93G reveals the importance of Ser 92 on the ligand off rate. The rate of Im exchange in S92A/H93G is identical to that in H93G, while ligand exchange is about two times slower in S92T/H93G. Thus, in S92A/H93G neither the loss of a hydrogen bond to the protein or the creation of a larger cavity affect the rate of ligand dissociation. On the other hand, the Im in S92T/H93G is less accessible to solvent, as demonstrated by proton exchange data, and this increases the barrier for ligand dissociation.

Imidazole Binding to Nitrosyl Complexes. Nitric oxide exerts a repulsive trans effect upon binding to ferrous hemes; in proteins such as guanylate cyclase, distal NO binding results in rupture of the proximal histidine−iron bond. As reported previously, binding constants of imidazoles to H93G−NO can be measured by a UV/vis titration technique (*6*); similar results have recently been reported for a cavity mutant in a β subunit fragment of guanylate cyclase (*3*).

N-MeIm binds to H93G−NO with a lower affinity than 4-MeIm. Since these two ligands have a similar size and pK_a, the difference in affinity was attributed to differences

[2] Unlike the study by Lecomte and La Mar, the proximal imidazole in the H93G mutants is not covalently attached to the polypeptide chain. Thus, one could propose an alternate mechanism to explain the saturation transfer data in these myoglobin cavity mutants in which proton exchange is coupled to ligand exchange, and the saturation transfer is measuring movement of the imidazole ligand in and out of the proximal cavity. However, data presented earlier (*5*) and in this paper demonstrate that Im exchange occurs much slower than the proton exchange rates, and such a mechanism could not explain the observed saturation transfer behavior. Thus, we believe that the standard base-catalyzed mechanism observed with the proximal histidine of wild-type myoglobin also applies to the proximal Im of the cavity mutants.

in hydrogen bonding with Ser 92 (*4*). In the double mutant S92A/H93G−NO, the binding constants for all of the imidazoles are much smaller than in H93G−NO; for example, *K* for Im is about 2 orders of magnitude smaller than in H93G and is close to the value observed in free heme−NO in detergent micelles (Belcher and Decatur, unpublished results). Moreover, in S92A/H93G−NO, *N*-MeIm and 4-MeIm have nearly the same binding affinity. Thus, we conclude that Ser 92 plays an important role in stabilizing Im binding to H93G−NO, that creation of a more open cavity in S92A/H93G lowers the binding constants of exogenous molecules, and that, in H93G−NO, *N*-MeIm is a poorer ligand than 4-MeIm because it lacks a hydrogen bond with Ser 92.

The binding constants for imidazoles to S92T/H93G−NO are very similar to, but slightly larger than, those in H93G-NO. The added size of threonine does not seem to have a large effect on the imidazole binding constants, but the more tightly packed and less accessible cavity does result in stronger affinity for Im and 4-MeIm.

Interestingly, the S92A mutation has a large effect on the binding constant of Im to the nitrosyl complex but no significant effect on the dissociation rate of Im from the metcyano complex. These contrasting results illustrate that *both iron−ligand bonding and ligand−protein interactions are important in modulating the binding properties of exogenous imidazoles to the proximal cavity*. When the bond between the iron and ligand is strong (as with Im−metcyanoheme interactions), the energy of the Ser 92−Im hydrogen bond is small relative to the barrier for ligand dissociation, and thus loss of that interaction does not impact the dissociation rate. However, when the bonding between the iron and the ligand is much weaker (as in the Im−nitrosylheme interactions), noncovalent interactions between the ligand and the protein cavity are very important in modulating ligand binding affinities.

ACKNOWLEDGMENT

We are very grateful to John Williams and Dr. Anne McDermott for a generous gift of 4,5-d_2 *N*-MeIm.

REFERENCES

1. Barrick, D. (1994) *Biochemistry 33*, 6545−6554.
2. DePillis, G. D., Decatur, S. M., Barrick, D., and Boxer, S. G. (1994) *J. Am. Chem. Soc. 116*, 6981−6982.
3. Zhao, Y., Hoganson, C., Babcock, G. T., and Marletta, M. A. (1998) *Biochemistry 37*, 12458−12464.
4. McRee, D. E., Jensen, G. M., Fitzgerald, M. M., Siegel, H. A., and Goodin, D. B. (1994) *Proc. Natl. Acad. Sci. U.S.A. 91*, 12847−12851.
5. Decatur, S. M., and Boxer, S. G. (1995) *Biochemistry 34*, 2122−2129.
6. Decatur, S. M., Franzen, S., DePillis, G. D., Dyer, R. B., Woodruff, W. H., and Boxer, S. G. (1996) *Biochemistry 35*, 4939−4944.
7. Decatur, S. M., DePillis, G. D., and Boxer, S. G. (1996) *Biochemistry 35*, 3925−3932.
8. Poulos, T. L., Freer, S. T., Alden, R. A., Edwards, S. L., Skogland, U., Takio, K., Eriksson, B., Xuong, N.-U., Yonetani, T., and Kraut, J. (1980) *J. Biol. Chem. 255*, 575−580.
9. Cheng, X., and Schoenborn, B. P. (1991) *J. Mol. Biol. 220*, 381−399.
10. Smerdon, S. J., Krzywda, S., Wilkinson, A. J., Brantley, R. E., Carver, T. E., Hargrove, M. S., and Olson, J. S. (1993) *Biochemistry 32*, 5132−5138.
11. Shiro, Y., Iizuka, T., Marubayashi, K., Ogura, T., Kitagawa, T., Balasubramanian, S., and Boxer, S. G. (1994) *Biochemistry 33*, 14986−14992.
12. Lloyd, E., Burk, D. L., Ferrer, J. C., Maurus, R., Doran, J., Carey, P. R., Brayer, G. D., and Mauk, A. G. (1996) *Biochemistry 35*, 11901−11912.
13. Wu, Y., Chien, E. Y. T., Sligar, S. G., and La Mar, G. N. (1998) *Biochemistry 37*, 6979−6990.
14. Peterson, E. S., Friedman, J. M., Chien, E. Y. T., and Sligar, S. G. (1998) *Biochemistry 37*, 12301−12319.
15. La Mar, G. N., and de Ropp, J. S. (1993) in *Biological Magnetic Resonance* (Berliner, L. J., and Reuben, Eds.) Vol. 12, pp 1−78, Plenum Press, New York.
16. Traylor, T. G., and Berzinis, A. (1980) *J. Am. Chem. Soc. 102*, 2844−2846.
17. Yamamoto, Y., Nanai, N., Chujo, R., and Suzuki, T. (1990) *FEBS Lett. 264*, 113−116.
18. Lecomte, J. T., and La Mar, G. N. (1985) *Biochemistry 24*, 7388−7395.
19. Sanders, J. K. M., and Hunter, B. K. (1992) *Modern NMR Spectroscopy*, 2nd ed., Oxford University Press, Oxford, U.K.
20. Cutnell, J. D., La Mar, G. N., and Kong, S. B. (1981) *J. Am. Chem. Soc. 103*, 3567−3572.
21. Lambright, D. G., Balasubramanian, S., and Boxer, S. G. (1989) *J. Mol. Biol. 207*, 289−299.
22. Mincey, T., and Traylor, T. G. (1979) *J. Am. Chem. Soc. 101*, 765−766.
23. Quinn, R., Mercer-Smith, J., Burstyn, J. N., and Valentine, J. S. (1984) *J. Am. Chem. Soc. 106*, 4136−4144.
24. Traylor, T. G., and Popovitz-Biro, R. (1988) *J. Am. Chem. Soc. 110*, 239−243.
25. Rajaratham, K., Qin, J., La Mar, G. N., Chiu, M. L., and Sligar, S. G. (1994) *Biochemistry 33*, 5495−5501.

BI9908888